An empirical formulation to describe the evolution of the high burnup structure

Martín Lemes, Alejandro Soba, Alicia Denis

PII: S0022-3115(14)00638-2
DOI: http://dx.doi.org/10.1016/j.jnucmat.2014.09.048
Reference: NUMA 48461

To appear in: *Journal of Nuclear Materials*

Received Date: 18 July 2013
Accepted Date: 21 September 2014

Please cite this article as: M. Lemes, A. Soba, A. Denis, An empirical formulation to describe the evolution of the high burnup structure, *Journal of Nuclear Materials* (2014), doi: http://dx.doi.org/10.1016/j.jnucmat.2014.09.048

AN EMPIRICAL FORMULATION TO DESCRIBE THE EVOLUTION OF THE HIGH BURNUP STRUCTURE

Martín Lemes, Alejandro Soba, Alicia Denis

Gerencia Ciclo del Combustible Nuclear,
Comisión Nacional de Energía Atómica,
Avenida General Paz 1499, 1650 San Martín, Provincia de Buenos Aires,
Argentina

Keywords: nuclear fuel, high burnup structure, porosity.

ABSTRACT

In the present work the behavior of fuel pellets for LWR power reactors in the high burnup range (average burnup higher than about 45 MWd/kgU) is analyzed. For extended irradiation periods, a considerable Pu concentration is reached in the pellet periphery (rim zone), that contributes to local burnup. Gradually, a new microstructure develops in that ring, characterized by small grains and large pores as compared with those of the original material. In this region Xe is absent from the solid lattice (although it continues to be dissolved in the rest of the pellet). The porous microstructure in the pellet edge causes local changes in the mechanical and thermal properties, thus affecting the overall fuel behaviour.

It is generally accepted that the evolution of porosity in the high burnup structure (HBS) is determinant of the retention capacity of the fission gases rejected from the fuel matrix. This is the reason why, during the latest years a considerable effort has been devoted to characterizing the parameters that influence porosity.

Although the mechanisms governing the microstructural transformation have not been completely elucidated yet, some empirical expressions can be given, and this is the intention of the present work, for representing the main physical parameters. Starting from several works published in the open literature, some mathematical expressions were developed to describe the behaviour and progress of porosity at local burnup values ranging from 60 to

300 MWd/kgU. The analysis includes the interactions of different orders between pores, the growth of the pore radius by capturing vacancies, the evolution of porosity, pore number density and overpressure within the closed pores, the inventory of fission gas dissolved in the matrix and retained in the pores. The model is mathematically expressed by a system of non-linear differential equations.

In the present work, results of this calculation scheme are compared with experimental data available in the open literature and with simulations performed by other authors. The results of these separate tests are quite satisfactory so, the next step will be the incorporation of this model as a new subroutine of the DIONISIO code, to expand the application range of this general fuel behaviour simulation tool.

1. INTRODUCTION

Numerous experimental research works [1,2,3,4,5,6,7,8] have revealed that when the average burnup of a nuclear fuel pellet exceeds a threshold of about 45 MWd/kgU, a typical morphology usually designed as *high burnup structure* (HBS) starts to form in the periphery of the UO_2 pellet, where the local burnup reaches more than about 60-70 MWd/kgU, and the temperature does not exceed about 1000ºC. The more outstanding characteristics can be summarized as follows:

- The original grain, of a typical size of about 10 μm, divides into 10^4 – 10^5 new grains of a typical size of 200 – 300 nm.
- Large faceted pores of a mean size of about 1μm are formed [9,10].
- The new grains have few dislocations and little gas in solid solution.
- The porosity can be one order of magnitude higher than in the original fuel material.
- The major part of the fission gas is confined at high pressure (200MPa) within the (large) pores.
- The modified structure occupies a thin layer in the pellet edge, the thickness of which can range from a few microns to about 300 μm for very high burnup levels.

- The new structure deteriorates the mechanical integrity of the pellet [1].
- The thermal conductivity of the pellet decreases with the local burnup, i.e. decreases towards the pellet edge [11].

Different authors [9,12] interpret that the recrystallization process starts with the formation of pores surrounded by a thin layer of small grains. The thickness of this layer increases as the burnup progresses until the layers surrounding neighboring pores make contact. At this point, the pore growth rate reduces and the region becomes completely recrystallized [9]. In the transition zone the local burnup is in the range from ≈60 MWd/kgU to ≈100 MWd/kgU. Beyond this burnup level, restructuring is complete.

The final purpose of this work is to develop a calculation tool adequate to be included in the fuel performance code DIONISIO. This code which was originally conceived to simulate normal operation conditions, has a modular structure and contains more than 40 interconnected models that simulate most of the main phenomena that take place within a fuel rod [13,14,15]. With the aim of extending the application range of the code, some subroutines that predict the radial distribution of power density, burnup and concentration of diverse nuclides within the pellet [16] were recently incorporated. These instruments, together with those developed in the present work, are expected to make DIONISIO capable of simulating high burnup conditions in a nuclear fuel rod.

With respect to the porosity model presented here, once it has been incorporated to DIONISIO as a new subroutine, the main program will provide it the input parameters in every iteration step, taking into account the great many interrelated phenomena in the fuel rod. Nevertheless, for the purpose of separately testing this porosity model, the values of some parameters need to be assigned. This is the case of: the porosity level reached after a local burnup of 60 MWd/kgU, which represents the initial value for this model; the hydrostatic pressure on the gas filled pores; the local value of temperature. In order to assign realistic values to the input parameters, experimental information obtained from the open literature was used.

2. MODEL

Porosity (volume fraction occupied by pores) and pore number density (number of pores per unit volume) deserve especial attention in the high burnup range, which can be conventionally considered to start at ≈60 MWd/kgU. Both properties show a change of behavior at a burnup threshold of about 100 MWd/kgU.

Porosity, which increases steadily as burnup progresses in the whole high burnup range, presents a quite definite change of growth rate at that threshold. In the interval between 60 and 100 MWd/kgU, porosity increases with burnup at a rate of about 1.7 % / 10 MWd/kgU until it reaches about 10% at the burnup critical value. For burnups higher than 100 MWd/kgU, the porosity increase rate drops to about 0.6 % / 10 MWd/kgU [3].

The pore number density, instead, increases with burnup until reaching a maximum of about 10^8 pores/mm^3 at 100 MWd/kgU and then decreases [3]. The change can be attributed to the increased probability of pores interlinkage (coalescence) [10,17]. For this reason, the description of the complete high burnup range is divided into two parts: *model one* deals with burnup levels between 60 and 100 MWd/kgU and *model two* with burnups higher than that threshold.

For burnup values markedly higher, the microstructure adopts an aspect designated in [18] as *ultra high burnup structure* (UHBS), characterized by the presence of extra large pores with mean sizes of ~7–8 μm in the very rim zone. J. Spino et al. [3] determined that even at a local burnup as high as 250 MWd/kgU pores percolation is not verified and the pores in the rim are expected to remain closed.

The porosity model presented here evaluates diverse pore parameters as functions of the local burnup. But, since the experimental data used to compare the results with are generally given as functions of the radius, some relation between the burnup and the radius is necessary. Once the subroutine has been incorporated to DIONISIO, the code will be able to provide this relationship starting from a number of parameters like the initial enrichment, the buildup of ^{239}Pu, the consumption of ^{235}U and the local linear power. But in the present calculation, aimed at making a separate test of the porosity model,

some mathematical expression is needed to represent the degree of burnup as a function of the radius. To this end, experimental data obtained with standard PWR fuel rods with 2.9 –5% enrichment that had reached high burnup levels [8,9] were chosen and the empirical relation (1) was fitted. With them, Figure 1 was drawn and the following empirical relation, valid for *Bu* in the high burnup range, was developed.

$$(1) \qquad \frac{r}{r_0} = \left[\frac{5}{6}\ln\left(\frac{Bu}{Bu_{av}}\right)\right]^{1/32} + 0.005 - 10^{-5}\ Bu_{av}$$

where Bu and Bu_{av} represent respectively the local and average burnup, measured in MWd/kgU, and r and r_{max} represent respectively the radial location and the pellet radius.

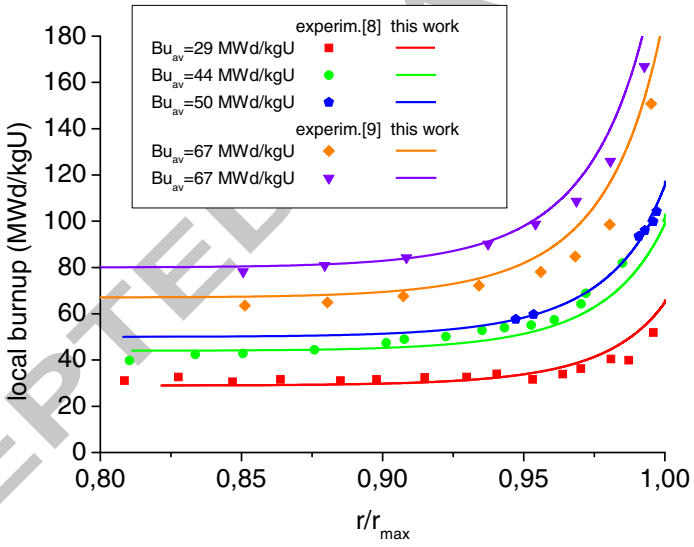

Figure 1: Experimental determinations [8,9] of local burnup vs. relative radial position and curve fitting according to eq. (1).

In the following formulation pores are assumed of spherical shape with uniform radius R_p. Porosity (σ) and pore density (n_p) are required to characterize the pore population within the material. These variables are related by

(2) $$\sigma = \frac{4}{3}\pi R_p^3 n_p$$

The accumulation of fission gas within the closed pores gives rise to an overpressure, $\Delta\zeta$, given by

(3) $$\Delta\zeta = P_p - \frac{2\gamma}{R_p} - P_h$$

where P_p is the pressure due to the gas within the pore, P_h is the hydrostatic pressure and γ is the surface energy of the pore, estimated as $\approx 1 J/m^2$ [17].

Experimental determinations [5,19] of the gas composition in the plenum obtained in LWR rods of different origin with standard enrichment, that had reached an average burnup of about 100 MWd/kgU, gave an atomic ratio of Xe/Kr~10.8 [20]. We assume here that the gas within the pores bears the same composition as the gas in the plenum and obeys the van der Waals equation.

(4) $$(P_p + \frac{a_{gas} N_p^2}{V^2})(V - b_{gas} N_p) = N_p kT$$

where N_p is the number of gas atoms in a pore of volume $V = \frac{4}{3}\pi R_p^3$, k is the Boltzmann constant and T is the absolute temperature. The van der Waals constants for the gas mixture were calculated as the weighted average of both gases: $a_{gas} = 1.12827 \times 10^{-48}$ m^{6}Pa/at^2 and $b_{gas} = 8.3214 \times 10^{-29}$m^3/at. Defining the concentration C_p (number of fission gas atoms enclosed in the pores per unit volume of the material) by $C_p = N_p n_p$, then (2) and (4) give

(5) $$[P_p + a_{gas}(\frac{C_p}{\sigma})^2](\sigma - b_{gas} C_p) = C_p kT$$

The hydrostatic pressure (P_h) is modified by factors like fuel swelling and the release of fission gas as burnup progresses [21]. Moreover, the existence of pellet-cladding contact also plays a role in the value of P_h. A simulation with DIONISIO provides at every calculation step all the variables necessary to determine the hydrostatic pressure. Nevertheless, given that the present calculation is intended to test separately the porosity predictions, a relationship between P_h and the burnup was provided to this end. The experimental results measured by [22] were chosen and the following empirical expression that involves all these factors was fitted

(6) $P_h = 0.07\,Bu + 1.8 + \lambda$ (MPa)

where $\lambda = 1$ when pellet-cladding contact exists and $\lambda = 0$ when it does not.

The fission gas generated during fuel irradiation is distributed among pores, matrix and rod free volume.

(7) $c_{gen} = c_p + c_{matrix} + c_{rel}$

where c_{gen}, c_p, c_{matrix} and c_{rel} are respectively the amount of gas generated, stored in the pores, dissolved in the fuel matrix and released to the free volume of the rod, all of them expressed as weight percent of fuel. The particular considerations made to evaluate each of them are described here below.

The fission yield of the different products (fraction of atoms generated per fission event) depends on several factors like the neutron spectrum and the nature of the isotope fissioned, and hence on the radial position within the pellet. However, following [1], for simplicity these aspects are not taken into account in the present analysis. Then, the production rate of gas in the fuel is assumed to be given by

(8) $$\frac{dc_{gen}}{dt} = y\,\dot{F}^{*}$$

where $\dot{F}^{*}$ represents the fission rate (number of fissions per unit volume and time) and the fission yield, *y*, of the gas atoms is assumed constant. Numerical

integration of (8) gives Δc_{gen} during each Δt. Equivalently, it can be expressed in terms of the burnup increase ΔBu verified during Δt. The proportionality constant (1.46×10^{-2}) proposed in [1] for Xe was modified to take into account the presence of Kr in the gas mixture in the ratio Xe/Kr~10.8

(9) $$\Delta c_{gen} = 1.595 \times 10^{-2} \Delta Bu \quad \text{wt\%}$$

The evaluation of c_{matrix} is based on the data and assumptions reported in [1] where, starting from experimental determinations performed on pellets irradiated up to average burnups between 40 and 73 MWd/kgU, an expression is derived there for the Xe concentration in the UO_2 matrix vs. the local burnup, as shown in Figure 2. Given the experimental uncertainty in the value of burnup corresponding to the initiation of microstructure transformation, several simulated curves are drawn corresponding to $Bu_0 = 50$, 55, 60, 65 and 70 MWd/kgU.

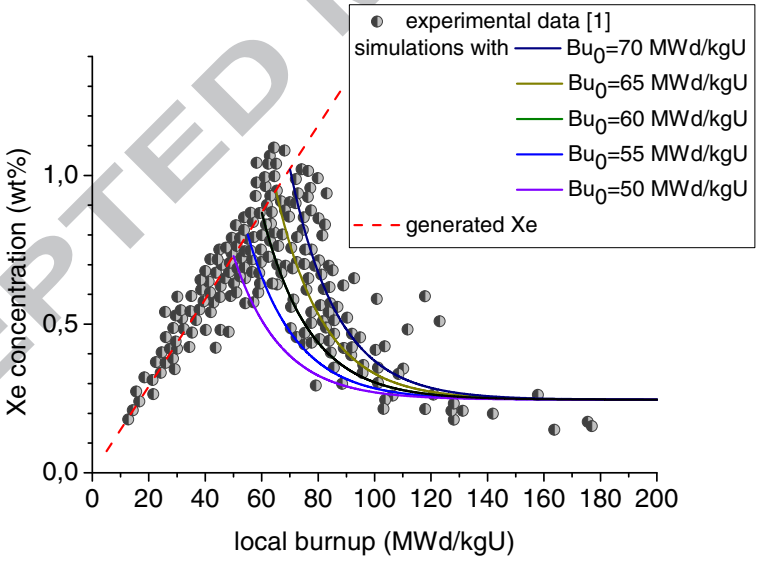

Figure 2: Concentration of Xe dissolved in the fuel matrix vs. local burnup; experimental data [1] and predictions obtained with equation (10) for different values of the burnup threshold.

To compute the presence also of Kr in the solid solution, the following expression was adopted for the total gas (Xe+Kr) dissolved in the fuel matrix, which is a slight modification of the formula derived in [1] for Xe,

(10) $$c_{matrix} = 1.595 \times 10^{-2} \left(\left(\frac{1}{\alpha} \right) + \left(Bu_0 - \left(\frac{1}{\alpha} \right) \right) e^{-\alpha (Bu - Bu_0)} \right) \text{ wt\%, for } Bu > Bu_0$$

where α is a fitting constant set equal to 0.058 so that, for high burnup levels, the gas concentration retained in the matrix tends towards the constant value 0.27 wt%, which corresponds to the observed content of Xe of ≈0.25 wt%.

Thus, c_p can be obtained from (7), (8), (9) and (10), along with c_{rel} that will be described in section 2.1. A simple calculation leads from c_p to C_p. This parameter, together with σ, has to be replaced in (5) to obtain P_p. The calculation of the porosity σ is also described in section 2.1.

Although the whole burnup range exhibits the global characteristics described at the beginning, as pointed out above some features show a different behaviour below and over the average burnup threshold of 100 MWd/kgU. Fitting parameters of models 1 and 2 are set so as to give a continuous junction of the curves that represent the model parameters as functions of the burnup.

In order to characterize the structural evolution of the pellet periphery once the high burnup regime is reached, several parameters of porosity are considered. The growth of overpressurized pores and the possible interactions between neighbouring ones are considered. This hypothesis is supported by the decrease in the pore number density that is observed when the burnup threshold is surpassed, with the concomitant appearance of a bi-(and also tri-)modal pore size distribution. The possibility of pore interaction with an open surface is also allowed in this modellization. This fact would lead to pore opening and venting its gas content to the free volume. The role of open surface, which is played by the grain boundaries during the initial burnup period (before restructuring), is played by the pellet external surface as long as the gap remains open. Given the rough character of the pellet and cladding surfaces, it can be conjectured that at least a fraction of the gap area remains open (and gap reopening is possible if the internal pressure increases sufficiently, for instance during a power ramp) for the duration of the first burnup period.

However, this possibility is impeded for sufficiently high burnup levels, when the pellet and cladding surfaces become bonded, as can be recognized in diverse micrographs of heavily irradiated rods [9,18,23,24]. In fact, as will be shown below, the calculations performed here predict that no pore venting takes place when the code is given reasonable values of the physical parameters.

2.1 Particular considerations for the first high burnup range

Experimental determinations [9] reveal that the pore fraction corresponding to open pores is very low in the burnup range corresponding to *model one*. In the present simulation c_{rel} was neglected.

On the basis of experimental data [3,25] of porosity vs. relative radius, and with the help of eq. (1), the following empirical expression was developed for porosity as a function of local burnup. It includes the possible effects of pellet-cladding mechanical interaction,

$$\sigma = \left[\frac{(0.025 - 0.008\lambda)Bu}{1 - 0.014 \times Bu + 5.9 \times 10^{-5} Bu^2}\right] - (0.03 - \sigma_0) \qquad (11)$$

σ_0 represents the porosity reached by the fuel material when $Bu = Bu_0 = 60$ MWd/kgU, i.e. when the high burnup range starts. Its value is usually in the range 3% to 7%, depending on the fabrication route and base irradiation conditions. Figure 3 shows the curves obtained from equation (11) for $\sigma_0 = 0.03$ and $\sigma_0 = 0.07$ respectively, with $\lambda = 1$, in comparison with points measured in experiments [3] where strong PCI has taken place. It is observed that most of the experimental points fall within the margins delimited by both curves. In Figure 5.d below, equation (11) is compared with data obtained with and without PCI, i.e. with $\lambda = 1$ and 0.

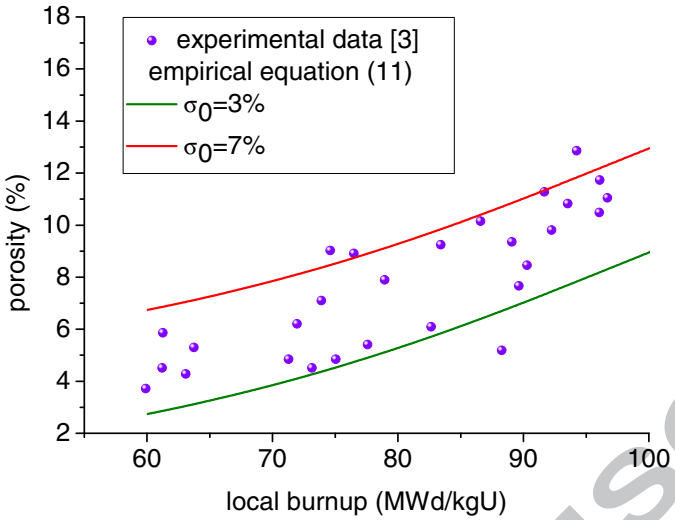

Figure 3: Experimental data of porosity [3] and curve given by formula (11)

In this burnup interval, the pore number density increases with the local burnup. Experimental data of the pore density vs. the radial position, measured in fuels with initial enrichment in the range 3.5-4.2% that had reached different average high burnup levels are reported in [9]. They are represented in Figure 4. An empirical formula was developed to fit these points. But, for later applications of this calculation scheme an expression relating the pore number density and the local burnup level is needed. Thus, the empirical formula (12) was developed

$$n_p = 0.45 \exp[(0.035 + \sigma_0/13)(Bu - 0.2Bu_{av})] \quad (12)$$

It includes the initial porosity and average burnup as parameters and is restricted to $Bu > Bu_{av}$. The curves plotted in Figure 4 were drawn for $\sigma_0 = 0.03$ and different values of the average burnup, using (12) along with (1) to relate the local burnup with the radial position (the conditions for which the latter was developed are also valid in the present cases).

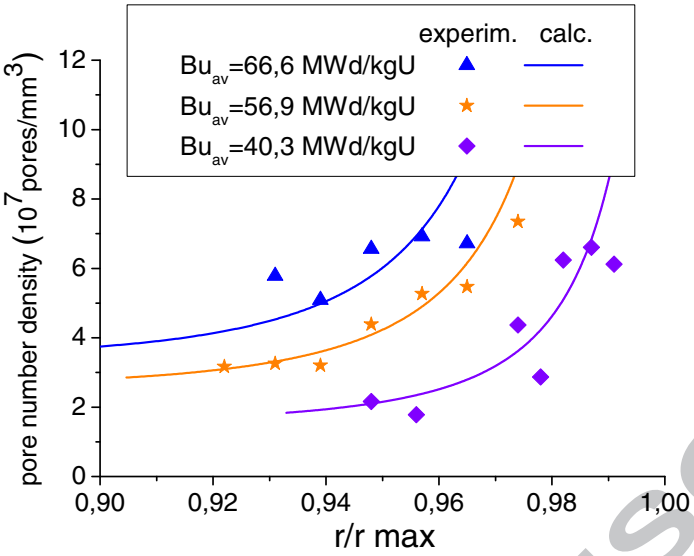

Figure 4: Experimental pore density data [9] and curve given by formula (12)

To determine the pore radius, equations (2), (11) and (12) are used:

$$R_p = \sqrt[3]{\frac{3\sigma}{4\pi n_p}}$$

2.2 Particular considerations for the second high burnup range

To describe the progress of the pores population a model is adopted that takes account of the mechanisms of pore growth due to trapping of vacancies and interstitials, of interactions of diverse orders between pores (and also allows, in principle, for the possibility of pore contact with the pellet surface).

With reference to the pore growth, it is generally accepted [10,17,26] that due to the pore overpressure a stress gradient is created around the pore that promotes the diffusion of point defects towards the pore. Although U and O defects are present in the fuel material, the rate limiting step for pore growth is the diffusion of uranium vacancies and interstitials. The pore radius grows at a rate given by [10,17,26]

$$(13) \qquad \frac{dR_p}{dt} = \frac{\Omega}{R_p}\left[D_v \Delta C_v - D_i \Delta C_i\right]$$

where Ω indicates the volume associated to the point defects assumed equal to the volume per uranium atom in the UO_2 lattice ($\Omega = 4.09 \times 10^{-29}\, m^3$). The

subscripts stand for vacancies and interstitials. $D_{v,i}$ are the respective diffusion coefficients. The quantities $\Delta C_{v,i} = C^0_{v,i} - C_{v,i}(R_p)$ represent the difference in the defects concentrations (number of vacancies/interstitials per unit volume) measured respectively on the pore surface, $C_{v,i}(R_p)$, and sufficiently far from it, $C^0_{v,i}$. Thermodynamic considerations yield for vacancies and interstitials

$$(14) \quad C_v = C_v^0 e^{-\frac{\Delta\zeta\Omega}{kT}} \qquad \text{and} \qquad C_i = C_i^0 e^{\frac{\Delta\zeta\Omega}{kT}}$$

The term $\Delta\zeta\Omega$ in both exponents represents the work invested to move an atom under a pressure $\Delta\zeta$ thus creating a point defect of volume Ω. The different signs are due to the volume change of the system in forming a vacancy or an interstitial. Substituting (14) in (13) and expressing the formula in terms of the fraction of sites occupied by vacancies/interstitials: $X_{v,i} = \Omega C_{v,i}$ we obtain

$$(15) \quad \frac{dR_p}{dt} = \frac{1}{R_p}[D_v X_v^0 (1 - \exp(-\frac{\Delta\zeta\Omega}{kT})) - D_i X_i^0 (1 - \exp(\frac{\Delta\zeta\Omega}{kT}))]$$

The factors $(1 - \exp(-\frac{\Delta\zeta\Omega}{kT}))$ and $(1 - \exp(\frac{\Delta\zeta\Omega}{kT}))$ express the balance of the populations of vacancies and interstitials due to thermal effects. The presence of irradiation induced defects is accounted for in the expressions for $D_{v,i}$ and $X^0_{v,i}$. Both parameters are analyzed here below.

To take into consideration the enhancement of diffusion due to irradiation, a term proportional to the fission rate $\dot{F}$ (fissions/m^{3}s) is added to the ordinary Arrhenius expression for the diffusion coefficient [10]

$$(16) \quad D_{v,i} = D^0_{v,i} \exp(-\frac{Q_{v,i}}{kT}) + a_{v,i}\dot{F}$$

In the Arrhenius term, the preexponential factors are $D_v^0 = 10^{-7}$ m^2/s and $D_i^0 = 10^{-8}$ m^2/s; the activation energies are $Q_v = 3.84 \times 10^{-19}$ J and

$Q_i = 3.20\times10^{-19}$ J [27]. The proportionality constants of the athermal terms were evaluated as $a_v = a_i = 1.2\times10^{-39}\,\mathrm{m}^5$ [10].

To calculate the fraction of point defects a balance equation is formulated for each species. Both equations include a term representing the production of Frenkel pairs: $zF\Omega$, where $z = 10^5$ [10] is the number of such pairs per fission event; a term describing the recombination of vacancies and interstitials: $\beta X_v X_i$ where the constant $\beta = \frac{4\pi l_{rec}}{\Omega} D_i$ is proportional to the recombination length $l_{rec} = 10^{-10}$ m [10] and to the diffusion coefficient of the uranium interstitials since the recombination rate is governed by the species that moves faster [28]; and finally, a term representing trapping of defects in the sinks present in the microstructure. In this respect and in agreement with P. Blair [10] we disregard the contributions of dislocations and grain boundaries to trapping of point defects. Hence, pores are assumed to be the single sinks for defects. According to Olander [17], the trapping rate for vacancies/interstitials at pores is given by $4\pi R_p n_p D_{v,i} X_{v,i}$. Combining the three terms, the rate of variation of the fractional concentrations of point defects is given by

(17) $$\frac{dX_v}{dt} = zF\Omega - \beta X_v X_i - 4\pi R_p n_p D_v X_v$$

(18) $$\frac{dX_i}{dt} = zF\Omega - \beta X_v X_i - 4\pi R_p n_p D_i X_i$$

The solution of this system of coupled differential equations gives the fractional concentrations of vacancies and interstitials that are substituted in (15) as X_v^0 and X_i^0 to yield the pore radius R_p.

The preceding equations assume an infinite medium, i.e. a material with isolated pores. However, for *Bu*>100 MWd/kgU, this assumption is no longer valid and hence the problem has to be formulated in a different manner.

When a local burnup of about 100 MWd/kgU or higher is reached, the radius of the closed pores is large enough to make plausible the contact

between two closed pores. The interlinking of closed pores, usually referred to as pores coalescence, gives rise to larger closed pores while the number of them decreases. Moreover, if the existence of an open surface is postulated, pore opening by contact with this surface can be assumed. (Within this description, it is assumed that, upon contact with the pellet surface, the gas content of a formerly closed pore instantly spills to the rod free volume). Also contact between a closed and an open pore, and interactions of higher order can be proposed.

To quantify the processes occurring in the vicinity of the pellet edge, the approach developed by G. Khvostov [10,26,29] was adopted. The method, originally conceived to give account of the fission gas behavior from the beginning of irradiation, is applied here in the high burnup range. It consists in evaluating the probabilities of interactions of diverse orders between closed pores, open pores and free surface, on the basis of geometrical considerations. The method provides a set of differential equations from which the rate of change of the number densities of closed and open pores, the gas content of the closed pores and the concentration of released gas can be evaluated.

3. RESULTS

The formulation presented above was compared with experimental data and with results of simulations performed with different codes, obtained in the specific literature.

The following three figures show the main parameters of the problem, i.e., porosity, pore number density, pore radius and fission gas concentration, as functions of the local burnup in the pellet.

In Figure 5 experimental determinations of porosity vs. local burnup obtained by different authors [3,25,30,31] are displayed. The points were measured at different radial positions in the periphery of pellets. In order to test the code predictions with these data, it is necessary to introduce the local temperature and the initial porosity, σ_0 (that attained at the end of the base irradiation) as input data. But the experimental determinations cannot provide these parameters for each measured point. Only reasonable estimations can be

given for both parameters in the restructured zone: the temperature in the range between 500 and 900K and the initial porosity between 3 and 5%.

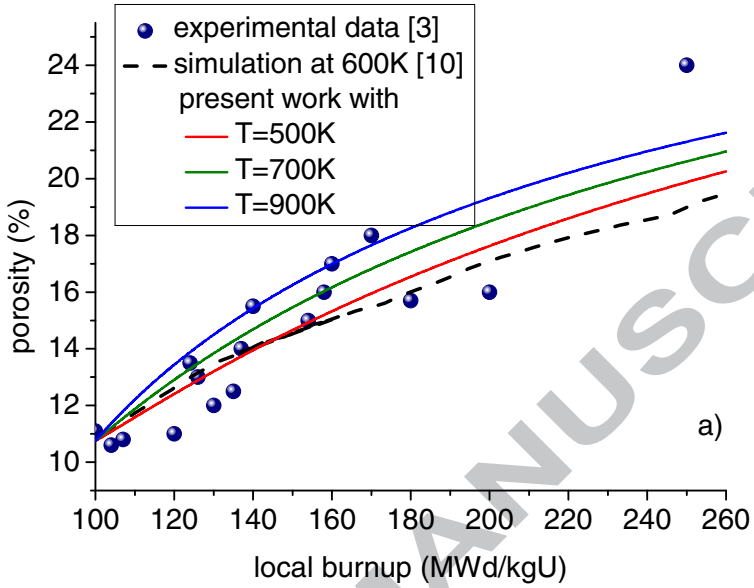

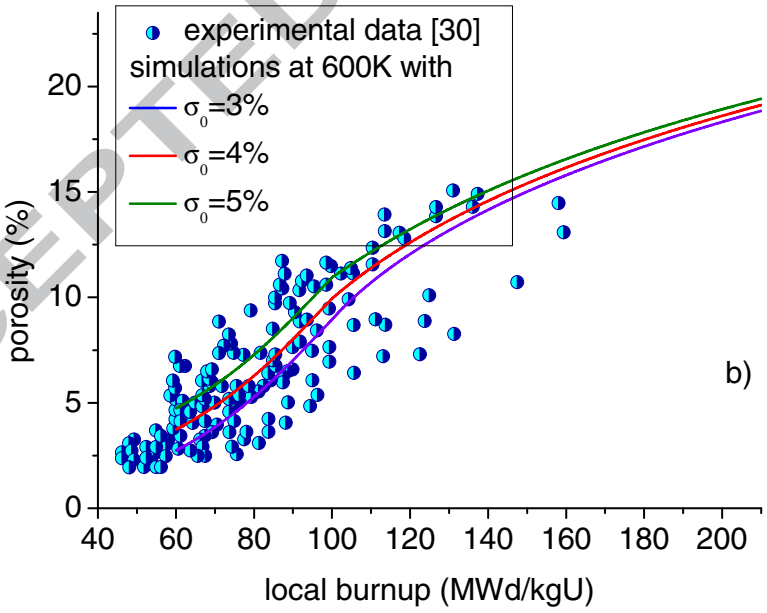

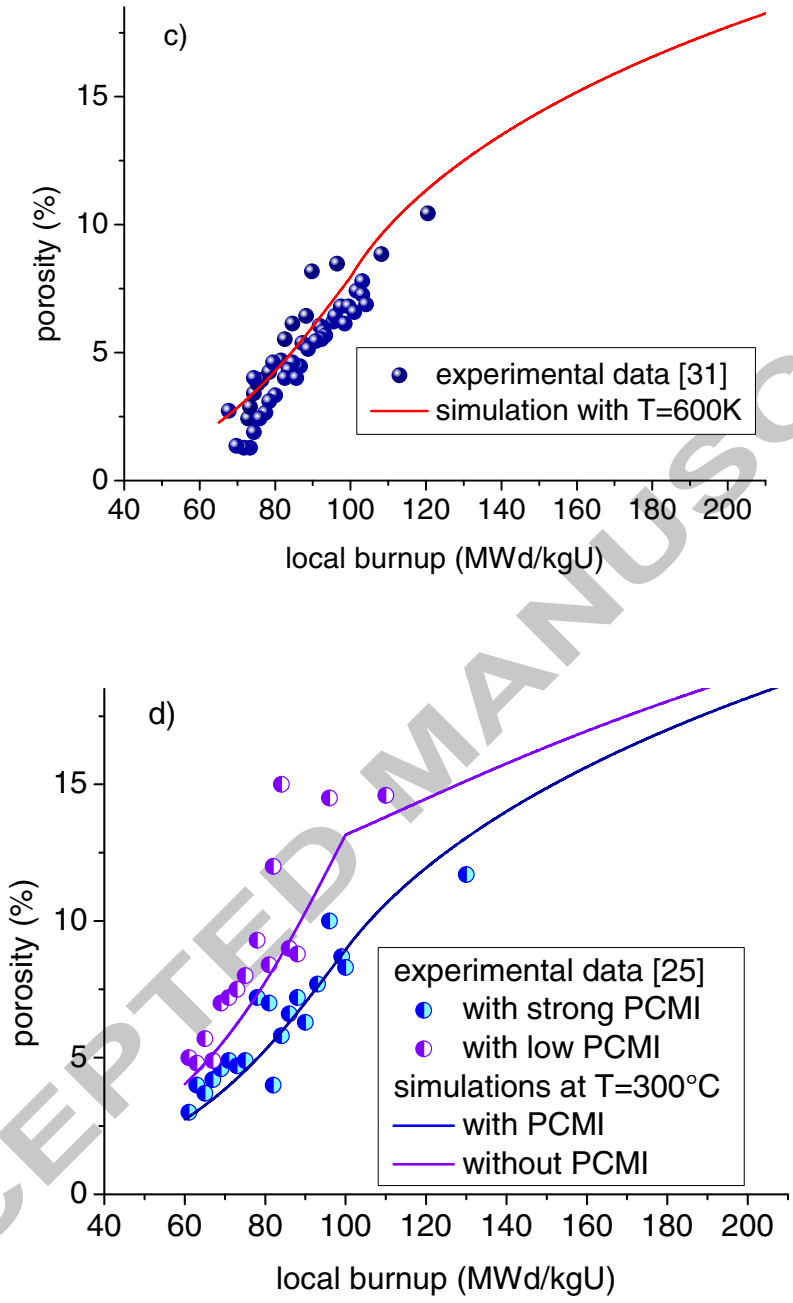

Figure 5: Total porosity vs. burnup. Comparison between the simulations performed with the present formulation and a) experimental results in [3] and a simulation reported in [10]; also with experimental results from b) [30], c) [31] and d) [25]

In Figure 5.a experimental data from ref. [3] corresponding to the range of *model two* along with a simulation carried out in [10] assuming a temperature of 600K are compared with calculations performed in the present work for

temperature values of 500, 700 and 900K. The initial porosity σ_0 was chosen so that at 100 MWd/kgU the calculated porosity reached a value of 11%, in coincidence with the curve reported in [10]. In Figure 5.b the experimental data reported in [30] are compared with simulations performed for T=600K, assuming initial porosities of 3, 4 and 5%. In like manner, Figure 5.c was plotted to compare the experimental data reported in [31] with simulations performed assuming a temperature of 600K and an initial porosity of 2.4%. Figure 5.d shows experimental values reported in [25] aimed at showing the effect of PCI on the evolution of porosity. In the range of *model one*, σ is calculated with equation (11). In Figure 5.d, the lower curve was obtained with λ=1 and the upper one with λ=0. The knee at the junction between models one and two is clearly recognized in the curves b, c and d.

Figure 6 shows experimental determinations of the pore number density and the average radius of closed pores performed by J. Spino et al. [3] superimposed with predictions of the model developed in this work.

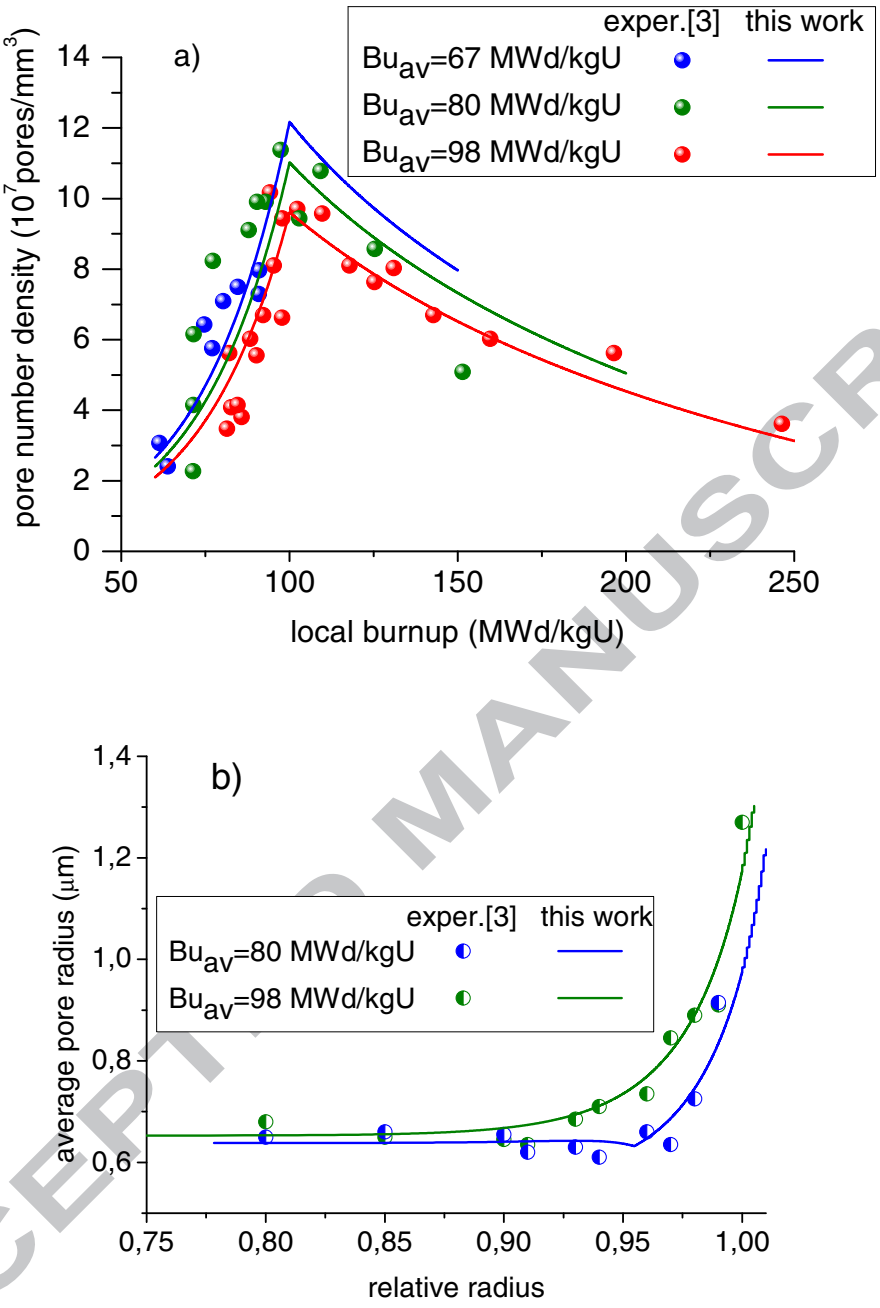

Figure 6: a) Pore number density vs. local burnup and b) average pore radius of closed pores vs. relative radial position in the pellet. Comparison between experimental results [3] and the simulations performed in this work

In Figure 7 the measurements performed by J. Spino et al. [32] of the total porosity as a function of the radial position in the pellet are plotted together with the simulations given by the present model. The experimental data correspond to LWR fuel pellets with average burnups of 40, 67, 97 and 102

MWd/kgU. The simulations were made assuming those values of average burnup, a temperature of 800 K and initial porosities of 2.5, 4, 6 and 9%, respectively.

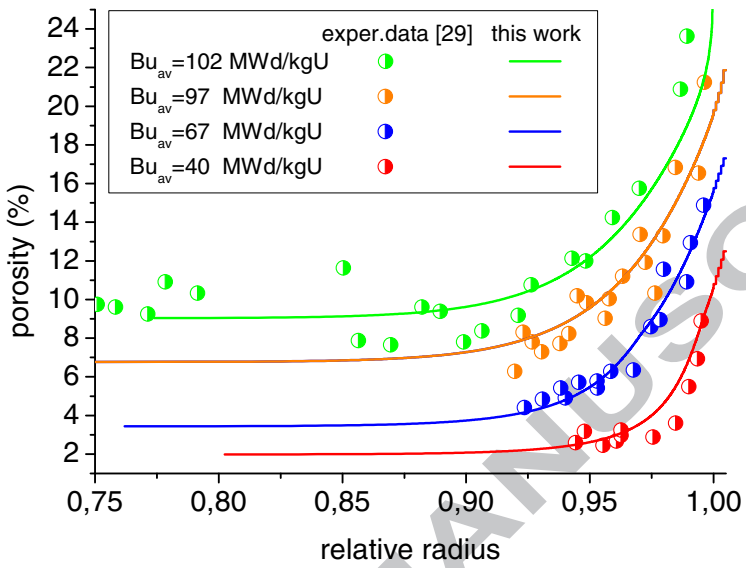

Figure 7: Comparison between experimental results [32] and the simulations performed with the present formulation for the total porosity vs. the relative radial position in the pellet.

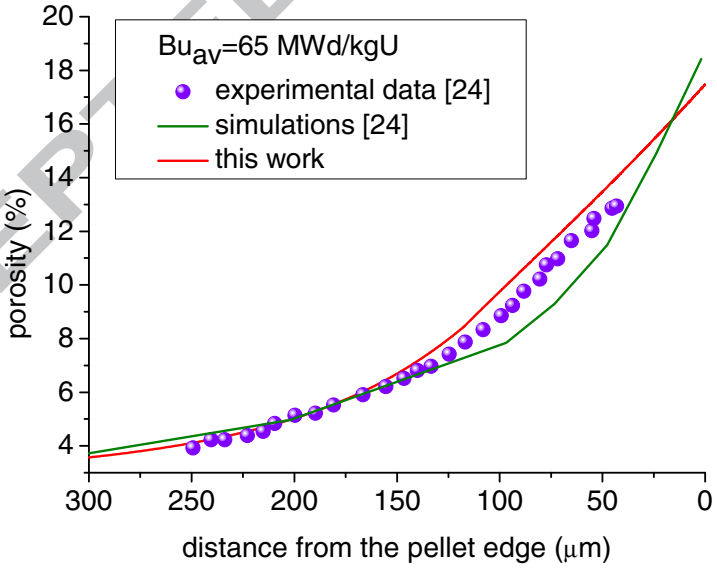

Figure 8: Experimental and simulated results of porosity reported in [24] are compared with the calculations performed with the present formulation vs. the radial position in the pellet measured from the external boundary.

Figure 8 shows experimental determinations and the result of a simulation reported by L. Noirot [24], along with the simulation performed in the present study for which an initial porosity of 2.5% was assumed. The data correspond to a sample with an average burnup of 65 MWd/kgU. In the horizontal axis the distance to the pellet edge is given in a decreasing scale so that the right limit corresponds to the pellet boundary.

Experimental and simulated values of the total porosity vs. the normalized radius reported respectively in [33] and [34] are presented in Figure 9 together with the simulations performed with the present model. The measurements were carried out on a sample that, after 9 irradiation cycles reached an average burnup of 97.8 MWd/kgU. An initial porosity of 7% and a temperature of 600ºC were assumed for the present calculations.

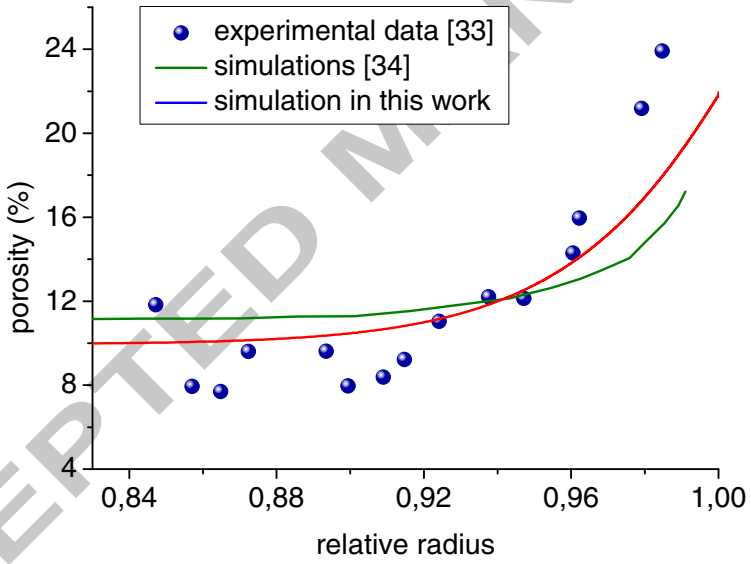

Figure 9: Comparison between experimental results [33], simulations reported in [34] and those obtained with the present formulation for the total porosity vs. the radial position in the pellet.

With reference to Figure 10, experimental determinations (by EPMA) of concentration of Xe retained in the UO_2 matrix and of total Xe contained in pores and matrix (by SIMS) reported by Walker et al. [20] are represented vs. the relative radial position (r / r_{max}) in the pellet. Simulations performed in the present work assuming a threshold burnup $Bu_0 = 50$ MWd/kgU, an average

burnup of 70 MWd/kgU and a temperature T=600K, are superimposed for comparison.

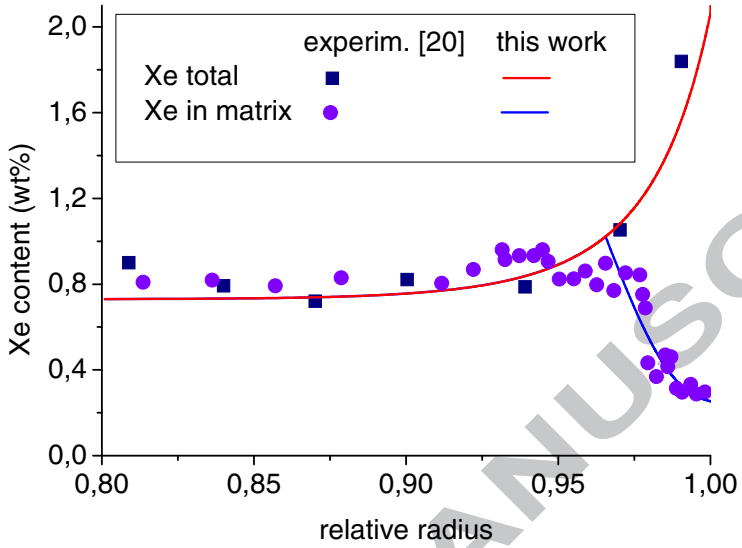

Figure 10: Comparison between the measured concentration of Xe dissolved in the fuel matrix [20] and the simulations performed in the present work

Figure 11 aims at showing that, although the present model allows for the existence of open porosity, the predictions lead to a negligible fraction of this type of pores when the model parameters are varied in a wide range of values. The closed and open porosities are plotted in a) vs. the relative radius for different levels of average burnup, assuming a uniform temperature of 700K and a porosity of 3% at the initiation of the HBS. In b) they are represented as functions of the local burnup for different initial porosities, assuming a uniform temperature of 700K and an average burnup of 60 MWd/kgU. It is seen that, in general, the open porosity is a small fraction, about 2–5x10^{-3}, of the closed porosity. Even at the very periphery of the pellet and for very high burnup levels (an average burnup of 90 MWd/kgU gives place to a local value of about 250 MWd/kgU at the pellet edge) the open porosity represents a volume fraction lower than 0.01% while the closed porosity is about 21%. These results agree quite well with those reported in [35] by Spino et al.

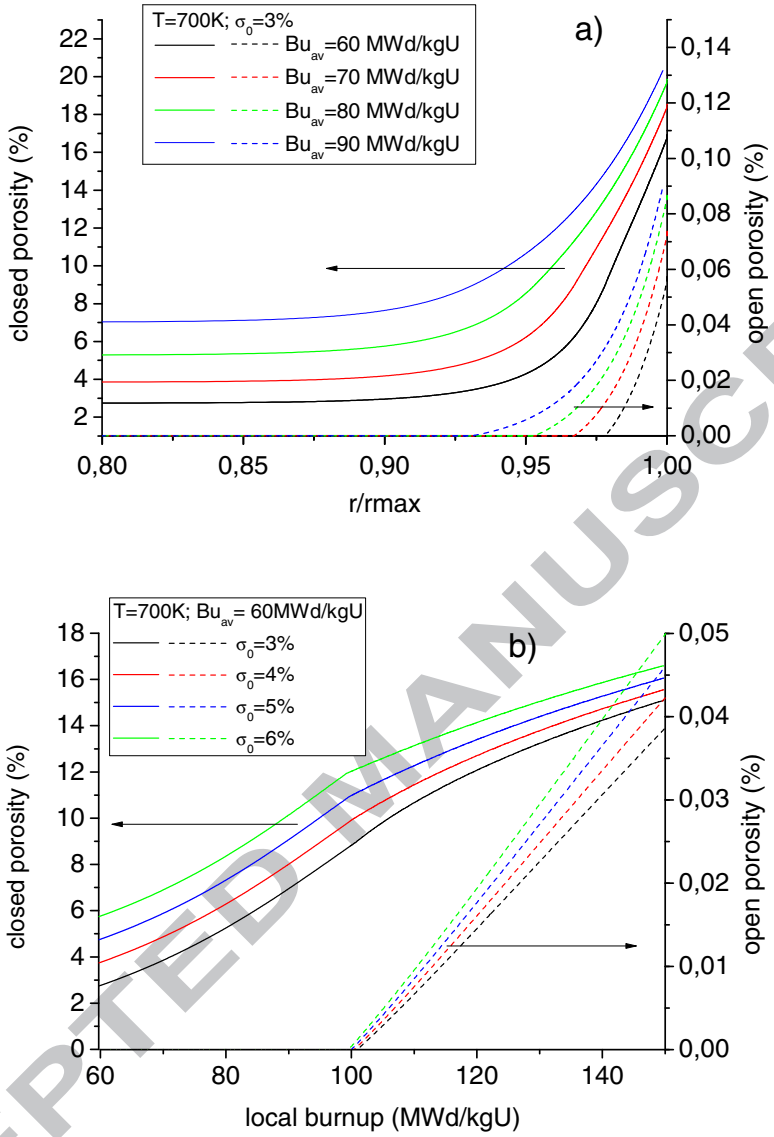

Figure 11: Distribution of closed and open porosity a) as functions of the radius, for different average burnups; b) as functions of the burnup, for different initial porosities

4. CONCLUSIONS

This work was oriented to develop a set of empirical expressions that could serve to describe as accurately as possible the process of formation and progress of the microstructure that characterizes of the high burnup range. The evolution of parameters like porosity and pore number densities of closed and open pores, overpressure of the fission gas within the closed pores, and concentration of point defects in the vicinity of these pores, as well as

inventories of gas retained in the solid matrix of the transformed pellet region, trapped in the pores and released to the rod free volume are considered in terms of the burnup, in the range between 60 and 300 MWd/kgU, as well as in terms of the radial position within the fuel pellet in its outer ring.

The formulation was subjected to numerous tests that included parametric analyses spanning a wide range of temperature, burnup, fission rate, surface/volume ratio, among others. The model testing also covered comparison of its results with experimental information available in the open literature and data of simulations performed with other similar codes.

The good quality of the predictions induces us to conclude that the general scheme and the regression formulae elaborated in this work are adequate. On this basis, a subroutine is to be incorporated to the DIONISIO code. With this addition the code, which was originally designed to simulate fuel behavior under normal irradiation conditions, is expected to expand its application range to the high burnup scenario.

REFERENCES

[1] K. Lassmann, C.T. Walker, J. van de Laar, F. Lindström, J. Nucl. Mater. 226 (1995) 1-8.
[2] Hj. Matzke, M. Kinoshita, J. Nucl. Mater. 247 (1997) 108-115.
[3] J. Spino, A. Stalios, H. Santa Cruz, D. Baron, J. Nucl. Mater. 354 (2006) 66–84.
[4] M. Kinoshita, T. Kameyama, S. Kitajima, Hj. Matzke, J. Nucl. Mater. 252 (1998) 71-78.
[5] R. Manzel, C.T. Walker, J. Nucl. Mater. 301 (2002) 170-182.
[6] N. Lozano, L. Desgranges, D. Aymes, J.C. Niepce, J. Nucl. Mat., 257 (1998) 78-87.
[7] J.P.Hiernaut, T. Wiss, J. Colle, H. Thiele, C.T. Walker, W. Goll, R. Konings, J. Nucl. Mater. 377 (2008) 313–324.
[8] K.Lassmann, C. O´Carroll, J. van de Laar, C.Walker, J. Nucl. Mater 208 (1994) 223-231
[9] J. Spino, K. Vennix, M, Coquerelle, J. Nucl. Mater. 231 (1996) 179-190.
[10] P. Blair, *Modelling of fission gas behaviour in high burnup nuclear fuel*, PhD Thesis, École Polytechnique Federale, Lausanne, Switzerland, 2008.
[11] C.T. Walker, D. Staicu, M. Sheindlin, D, Papaioannou, W. Goll, F, Sontheimer, J. Nucl. Mater. 350 (2006) 19-39.
[12] Hj. Matzke, J. Nucl. Mater. 189 (1992) 141-148.
[13] A. Soba, A., *Simulación del comportamiento termomecánico de una barra combustible en operación*, PhD Thesis, FCEyN, Universidad *de* Buenos Aires (2007).
[14] A. Denis, A. Soba, Nucl. Engin. Des. 223 (2003) 211-229.
[15] A. Soba, A. Denis, J. Nucl. Mater. 374 (2008) 32-43.
[16] A. Soba, A. Denis, L. Romero, E. Villarino, F. Sardella, J. Nucl. Mater. 433 (2013) 160-166.
[17] D. Olander, *Fundamental aspects of nuclear reactor fuel elements*, Department of Nuclear Engineering, University of California, Berkeley, 1976.
[18] A. Romano, M, Horvath, R. Restani, J. Nucl. Mater. 361 (2007) 62-68.
[19] K.Lassmann, A.Schubert, J.van de Laar, C.Vennix. *Recent developments of the TRANSURANUS code with emphasis on high burnup phenomena.* IAEA-TECDOC—1233. 2001.
[20] C.T. Walker, S. Bremier, S. Portier , R. Hasnaoui, W. Goll, J. Nucl. Mater. 393 (2009) 212-223.

[21] M. Suzuki, Nucl. Engin. Des. 201 (2000) 99–106.
[22] S. Motoe, J. Nucl. Mater., 201 (2000) 99-106.
[23] J. Spino, D. Baron, M. Coquerelle, A. Stalios, J. Nucl. Mater. 256 (1998) 189-196
[24] J. Noirot, J. Nucl. Sci. Tech., 43 (2006) 1149–1160.
[25] K. Une, K. Nogita, T. Shiratori, K. Hayashi, J. Nucl. Mater. 288 (2001) 20-28.
[26] G. Khvostov, K. Mikityuk, M. Zimmermann, Nucl. Engin. Des. 241 (2011) 2983-3007.
[27] M. Kinoshita, J. Nucl. Mater., 248 (1997) 185-190.
[28] J. Griesmeyer, N, Ghoniem, J. Nucl. Mater. 80 (1979) 88-101.
[29] P. Blair, G. Khvostov, A. Romano, Ch. Hellwig, R. Chawla, J. Nucl. Sci. Tech., 45 (2008) 639-646.
[30] K. Lassmann, A. Schubert, J. Van De Laar, International Conference on Nuclear Fuel for Today and Tomorrow, 2003.
[31] J. Noirot, L. Desgranges, J. Lamontagne, J. Nucl. Mater. 372 (2008) 318-339.
[32] J. Spino, J. Rest, W. Goll, C.T. Walker, J. Nucl. Mater. 346 (2005) 131-144.
[33] R.Manzel, C.T.Walker, Proc. ANS Topical Meeting on Light Water Reactor Fuel Performance, Park City, Utah, 2000
[34] L.Jernkvist, A.Massih, SKI report 2005:41, Quantum Technology, Uppsala, Sweden, 2004.
[35] J.Spino, D. Papaioannou, J.Glatz, J. Nucl. Mater. 328 (2004) 67-70.